Three-dimensional finite element modelling of sealed and unsealed roads considering effects of moving wheel loads

Piyush Punetha [1][0000-0002-0812-4708] and Sanjay Nimbalkar [1][0000-0002-1538-3396]

[1] School of Civil and Environmental Engineering, University of Technology Sydney, Australia
Sanjay.Nimbalkar@uts.edu.au

Abstract. Accurate simulation of the response of sealed and unsealed roads to moving wheel loads is essential for improving the current understanding of their behaviour. A proper evaluation of the stress distribution within different pavement layers under moving loads is essential for their appropriate design. This article presents the findings of three-dimensional (3D) finite element (FE) analyses carried out on sealed and unsealed roads, taking into account the effects of moving wheel loads. A parametric study is conducted to investigate the influence of variables, such as the elastic modulus of pavement layers, on the performance of both sealed and unsealed roads. The results reveal that the peak values of vertical stress at the subgrade top under moving wheel load are more sensitive to the base modulus for the unsealed road than the sealed roads, which is due to the structural difference between the two road types. The results predicted using FE models are also compared with those from the approach commonly used by practising engineers. The findings from this study demonstrate the capability of 3D FE method in evaluating critical responses of sealed and unsealed roads under moving wheel loads, which are crucial for optimising their design.

Keywords: Finite Element Modelling, Sealed Road, Unsealed Road.

1 Introduction

The flexible pavements are intricately complex systems whose performance depends on factors such as material properties, environmental conditions, vehicular loads and construction methods [1]. The accurate evaluation of the response of these pavements subjected to moving vehicular loading is crucial for their proper design. Consequently, there have been several attempts in the past to monitor their performance in the field [e.g., 2, 3-6] and testing facilities [e.g., 7, 8, 9]. Apart from these investigations, numerical simulation is emerging as a viable option for assessing and analysing the geotechnical characteristics of flexible pavements, contributing to their effective design.

Several researchers have employed the two-dimensional (2D) finite element (FE) method to evaluate the performance of sealed roads under vehicular loading [e.g., 10, 11]. Although the 2D FE method is simple, requires low computational effort and relatively less time than the three-dimensional (3D) FE method, it is unable to simulate the 3D loading due to moving vehicles. Therefore, 3D finite element models of flexible pavements have been developed recently for evaluating their mechanical behaviour [e.g., 12, 13-17]. The moving vehicular loading in the past studies was primarily simulated using equivalent approaches, which include the application of time-varying stress pulses on rectangular loading area [12, 15] or shifting of tyre loading imprint over the loaded area (also termed quasi-static approach) [13, 14]. However, investigations involving the simulation of actual wheel translation and tyre-pavement contact behaviour are relatively scarce. In addition, most of these analyses dealt with the performance of the sealed roads, and studies focusing on the response of unsealed roads under moving vehicular loading are limited.

This study investigates the critical response of sealed and unsealed roads under moving wheel loads using 3D FE analyses. Moving vehicular loading is applied by translating rectangular plates while simulating the interaction between tyre and pavement. The accuracy of the results is verified by comparing the predictions with those computed using the software CIRCLY [18]. A parametric analysis is conducted to evaluate the sensitivity of critical pavement response to variations in the elastic modulus of the base, subbase, and subgrade layers.

2 Model development

Fig. 1 shows the 3D models of sealed and unsealed roads developed using the FE software ABAQUS [19]. The sealed road comprises 150 mm thick base and subbase courses overlying a 3,000 mm thick subgrade. It must be noted that the base layer (130 mm thick) and sprayed seal layer (20 mm thick) are represented in the FE model as one layer with a combined thickness of 150 mm. This is because a thin sprayed seal is used to minimise moisture ingress and has a negligible contribution to the load-carrying capacity of the road [20]. The unsealed road comprises a 150 mm thick base course overlying a 3,000 mm thick subgrade. The length of the model along both the longitudinal (y) and transverse (x) directions is taken as 10 m to avoid boundary effects. A single axle dual tyre assembly has been considered, which applies a vertical load of 80 kN on the top of the pavement. The moving load has been simulated by translating rectangular plates (each representing tyre-pavement contact) on the top of the pavement along the y direction. The dimensions of the plates are selected such that the tyre-pavement contact pressure is 750 kPa (see **Fig. 1** and [21]). The tyre-pavement interface behaviour is simulated using the Coulomb friction model available in ABAQUS [19].

Only one-half of the pavement is modelled owing to the symmetry. Standard boundary conditions are applied to the model, i.e., the nodes along the bottom boundary are fixed (i.e., restricted movement along vertical, lateral, and longitudinal directions), while the nodes along the side boundaries are normally supported (i.e., their movement is restricted only in horizontal direction, and they are free to move along vertical direction). Both the models are discretised using 8-noded 3D brick elements (C3D8R), and the entire assembly comprises 334,032 and 369,756 elements for unsealed and sealed roads, respectively. The number of elements is decided based on the findings of the mesh sensitivity analysis.

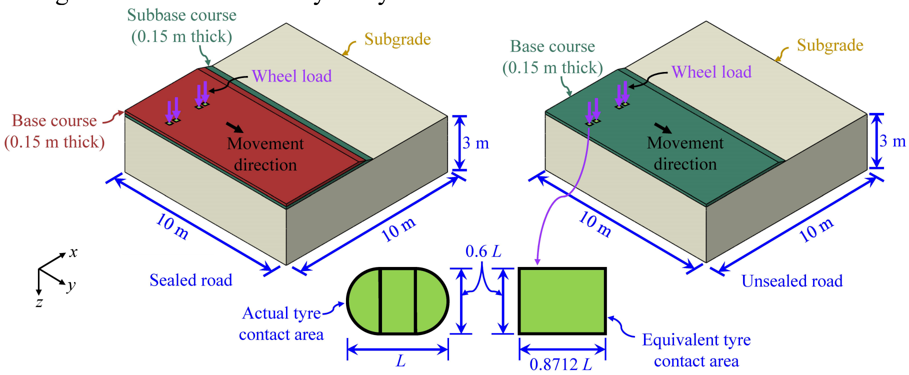

Fig. 1. 3D FE models of sealed and unsealed roads.

Table 1 lists the material properties used in the numerical simulations. These values are selected based on the published literature and engineering judgement. The base, subbase and subgrade layers are considered linear-elastic materials.

Table 1. Material properties used in the numerical simulations.

Property	Sealed road		Unsealed road	Subgrade
	Base	Subbase	Base	
Density, ρ (kg/m^3)	2,245	2,190	2,190	2,160
Elastic modulus, E (MPa)	200† – 500†	150† – 400†	150† – 400†	10$^\#$ – 140
Poisson's ratio, v	0.35†	0.35†	0.35†	0.4

Note: Values sourced from: †[22]; $^\#$[23].

3 Validation of 3D finite element model

The results predicted from the FE analyses are compared to those computed using the multilayer elastic theory-based software CIRCLY [18], which is routinely used by pavement engineers in Australia. It is worth mentioning that CIRCLY assumes a circular contact area between tyre and pavement. In contrast, a rectangular tyre-pavement contact area is adopted in ABAQUS. **Fig. 2** and **Fig. 3** depict the variation of vertical stress with depth predicted using ABAQUS and CIRCLY for unsealed and sealed roads, respectively. It is apparent that the stresses predicted using ABAQUS are in close agreement with those computed using CIRCLY for both type of roads, thus verifying the accuracy of the results from the FE analysis. Slight deviations in the results may be attributed to different tyre-pavement contact shapes considered in the two methods.

4 Results and discussion

A parametric investigation is conducted to understand the behaviour of sealed and unsealed roads when the elastic modulus of the pavement layers (base, subbase, and subgrade) is varied. The range of parameters used in the simulation is provided in **Table 1**. The nominal values of the elastic modulus for the base and subbase layers for the sealed road are 200 MPa and 150 MPa, respectively. The nominal values for the base layer of the unsealed road and subgrade are considered 150 MPa and 140 MPa, respectively.

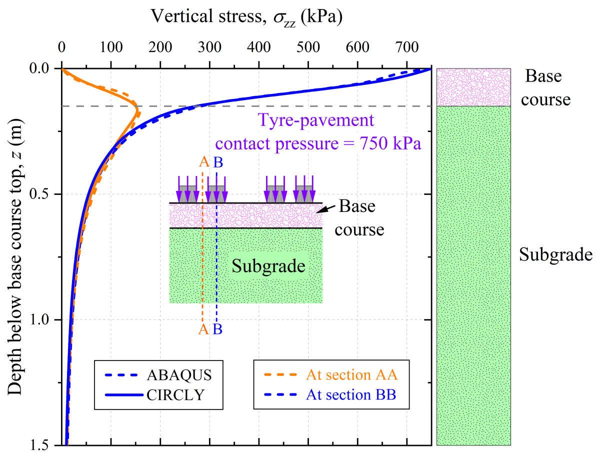

Fig. 2. Variation of vertical stress with depth predicted using ABAQUS and CIRCLY for unsealed road.

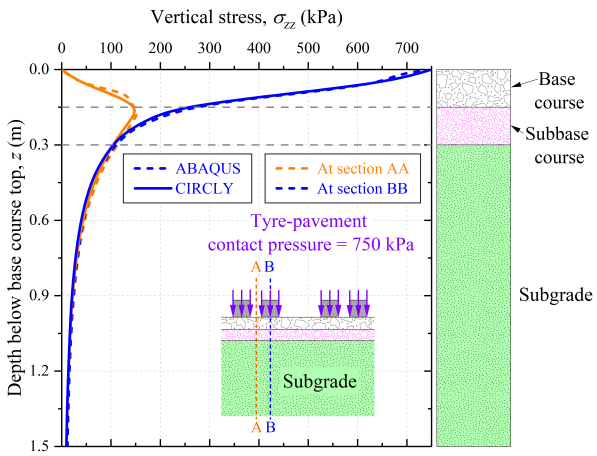

Fig. 3. Variation of vertical stress with depth predicted using ABAQUS and CIRCLY for sealed road.

Fig. 4 shows the variation of peak vertical stress (σ_{zz}) at the subgrade top with the base modulus (E_b) at different subgrade modulus (E_g) values for the unsealed road. It is apparent from the figure that σ_{zz} decreases with an increase in E_b. This reduction is attributed to the higher stress-spreading ability of stiffer base layer. It can also be observed that σ_{zz} increases with an increase in E_g. For instance, σ_{zz} at E_b = 150 MPa increases by 127% as E_g increases from 10 MPa to 140 MPa. Thus, the results demonstrate the importance of providing a stiffer base layer for reducing the stresses at the subgrade top for the unsealed roads.

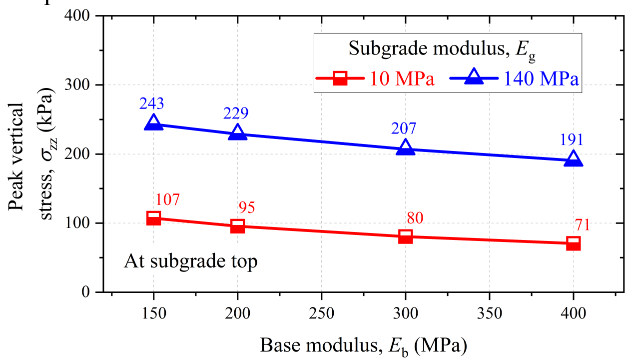

Fig. 4. Variation of peak vertical stress at the subgrade top with base modulus for unsealed road.

Fig. 5 shows the variation of σ_{zz} at the subgrade top with E_b at different subbase modulus (E_s) values for the sealed road. It is apparent that σ_{zz} at the subgrade top decreases with an increase in E_b and E_s. This reduction is reasonable since the stiffer (i.e., with higher elastic modulus values) base and subbase layers have a greater stress-spreading ability.

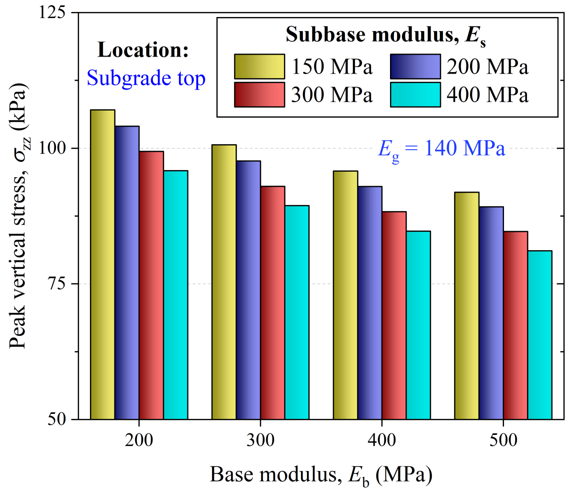

Fig. 5. Variation of peak vertical stress at subgrade top with base modulus for sealed road.

A sensitivity analysis is also performed to determine the effects of change in E_b (and E_s) on σ_{zz} at the subgrade top for both unsealed and sealed roads. The level of sensitivity (s) is computed as the ratio of the percentage change in σ_{zz} to the percentage change in E_b or E_s.

Fig. 6 illustrates the results of the sensitivity analysis, which reveals that σ_{zz} is more sensitive to the changes in E_b (s ranging between 0.09 and 0.13) as compared to E_s (s ranging between 0.06 and 0.09) for the sealed roads. It is also evident from the figure that σ_{zz} at the subgrade top for the unsealed road (s ranging between 0.13 to 0.18) is more sensitive to E_b as compared to the sealed road. This is due to the difference in the pavement structure, as the sealed road includes 150 mm thick base and subbase layers; however, the unsealed road consists of only a 150 mm thick base layer, above the subgrade.

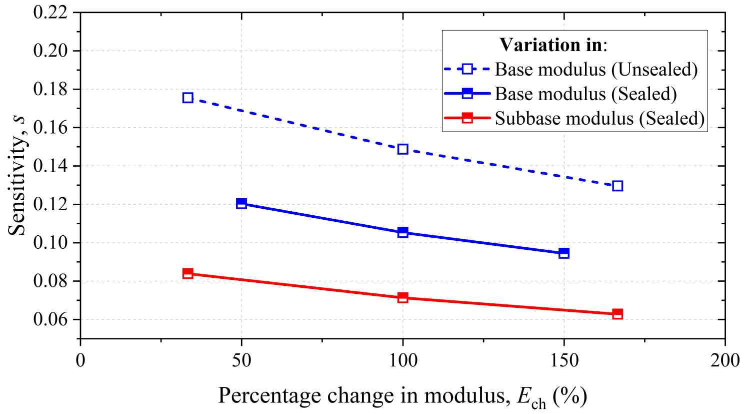

Fig. 6. Results of sensitivity analysis.

5 Conclusions

This paper presents the results of the FE analyses on unsealed and sealed roads to evaluate their response under moving loads. The results revealed that the peak vertical stress at the subgrade top decreases with an increase in base modulus for both sealed and unsealed roads. The peak values of vertical stress at the subgrade top under moving wheel load are found to be more sensitive to the base modulus in the case of the unsealed road than the sealed road. This is attributed to the structural difference in these roads, as the sealed road comprised 150 mm thick base and subbase layers, whereas the unsealed road comprised only a 150 mm thick base layer, above the subgrade. In addition, the subgrade stress for the sealed roads is more sensitive to changes in the base modulus than that of the subbase modulus. These findings demonstrate the effectiveness of the 3D FE method in assessing the critical responses of both sealed and unsealed roads under moving loads, which are vital for their design optimisation.

Acknowledgements

The authors greatly appreciate the financial support provided by SmartCrete CRC and the industry partners (Scenic Rim Regional Council and Queensland Department of Environment and Science) through the 21.PP.0120 project for conducting this research. The authors also thank the anonymous reviewers for their comments and suggestions.

References

1. Helwany, S., Dyer, J., Leidy, J.: Finite-element analyses of flexible pavements. Journal of Transportation Engineering 124(5), 491-499 (1998).
2. Al-Qadi, I.L., Loulizi, A., Elseifi, M., Lahouar, S.: The Virginia Smart Road: The Impact of Pavement Instrumentation on Understanding Pavement Performance. Journal of the Association of Asphalt Paving Technologists 73(3), 427-465 (2004).
3. Swett, L., Mallick, R.B., Humphrey, D.N.: A study of temperature and traffic load related response in different layers in an instrumented flexible pavement. International Journal of Pavement Engineering 9(5), 303-316 (2008).
4. Xue, W. Weaver, E.: Pavement Shear Strain Response to Dual and Wide-Base Tires. Transportation Research Record 2225(1), 155-164 (2011).
5. Maadani, O., Abd El Halim, A.O., Mostafa, N.: Instrumentation for Monitoring Pavement Performance in Cold Regions. Journal of Cold Regions Engineering 29(4), 04014017 (2015).
6. Blanc, J., Hornych, P., Duong, N.S., Blanchard, J.-Y., Nicollet, P.: Monitoring of an experimental motorway section. Road Materials and Pavement Design 20(1), 74-89 (2017).
7. Kim, I.T. Tutumluer, E.: Field Validation of Airport Pavement Granular Layer Rutting Predictions. Transportation Research Record 1952, 48–57 (2006).
8. Arraigada, M., Partl, M.N., Angelone, S.: Determination of Road Deflections from Traffic Induced Accelerations. Road Materials and Pavement Design 8(3), 399-421 (2011).
9. Kang, M., Wang, H., Qamhia, I.I.A., Tutumluer, E., Garg, N., Villafane, W., Murrell, S.: Evaluation of Airport Pavement Base Layer Stiffness Characteristics via Embedded Field Sensors. Transportation Research Record 2677(8), 462–473 (2023).
10. Kettil, P., Lenhof, B., Runesson, K., Wiberg, N.E.: Simulation of inelastic deformation in road structures due to cyclic mechanical and thermal loads. Computers & Structures 85(1), 59-70 (2007).
11. Ali, B., Sadek, M., Shahrour, I.: Finite-Element Model for Urban Pavement Rutting: Analysis of Pavement Rehabilitation Methods. Journal of Transportation Engineering 135(4), 235-239 (2009).

12. Saad, B., Mitri, H., Poorooshasb, H.: Three-Dimensional Dynamic Analysis of Flexible Conventional Pavement Foundation. Journal of Transportation Engineering 131(6), 460-469 (2005).
13. Elseifi, M.A., Al-Qadi, I.L., Yoo, P.J.: Viscoelastic Modeling and Field Validation of Flexible Pavements. Journal of Engineering Mechanics 132(2), 172–178 (2006).
14. Wang, H. Al-Qadi, I.L.: Combined Effect of Moving Wheel Loading and Three-Dimensional Contact Stresses on Perpetual Pavement Responses. Transportation Research Record 2095(1), 53-61 (2009).
15. Ghadimi, B., Nikraz, H., Rosano, M.: Dynamic simulation of a flexible pavement layers considering shakedown effects and soil-asphalt interaction. Transportation Geotechnics 7, 40-58 (2016).
16. Li, P., Liu, J., Zhao, S.: Implementation of stress-dependent resilient modulus of asphalt-treated base for flexible pavement design. International Journal of Pavement Engineering 19(5), 439-446 (2018).
17. Pooni, J., Robert, D., Giustozzi, F., Setunge, S., Venkatesan, S.: Stabilisation of expansive soils subjected to moisture fluctuations in unsealed road pavements. International Journal of Pavement Engineering 23(3), 558-570 (2020).
18. Mincad Systems: CIRCLY7 for Mechanistic Pavement Design and Analysis (Version 7.0). Mincad Systems Pty Ltd, Victoria, Australia (2017).
19. Dassault Systèmes: Abaqus (Version 2018). Dassault Systèmes Simulia Corp, Providence, RI (2018).
20. Saleh, M.F., Steven, B., Alabaster, D.: Three-Dimensional Nonlinear Finite Element Model for Simulating Pavement Response: Study at Canterbury Accelerated Pavement Testing Indoor Facility, New Zealand. Transportation Research Record 1823(1), 153-162 (2003).
21. Huang, Y.H.: Pavement Analysis and Design. Pearson Prentice Hall, New Jersey, USA (2004).
22. Austroads: Guide to Pavement Technology Part 2: Pavement Structural Design. Austroads, Sydney, Australia (2017).
23. Sharp, R.W. Booker, J.R.: Shakedown of pavements under moving surface loads. Journal of Transportation Engineering 110(1), 18521 (1984).